PNAS
www.pnas.org

Supporting Information for:

Macroscale intrinsic network architecture of the hypothalamus.

Joel D. Hahn, Olaf Sporns, Alan G. Watts, and Larry W. Swanson

Corresponding author 1:
Joel D. Hahn
Email: joelhahn@usc.edu

Corresponding author 2:
Larry W. Swanson
Email: larryswanson10@gmail.com

This PDF file includes:

Fig. S1, S2, S3, S4, S5
Captions for Datasets S1, S2, S3
References for SI reference citations

Additional supporting information for this manuscript includes the following:

Datasets S1, S2, S3

www.pnas.org/cgi/doi/10.1073/pnas.1819448116

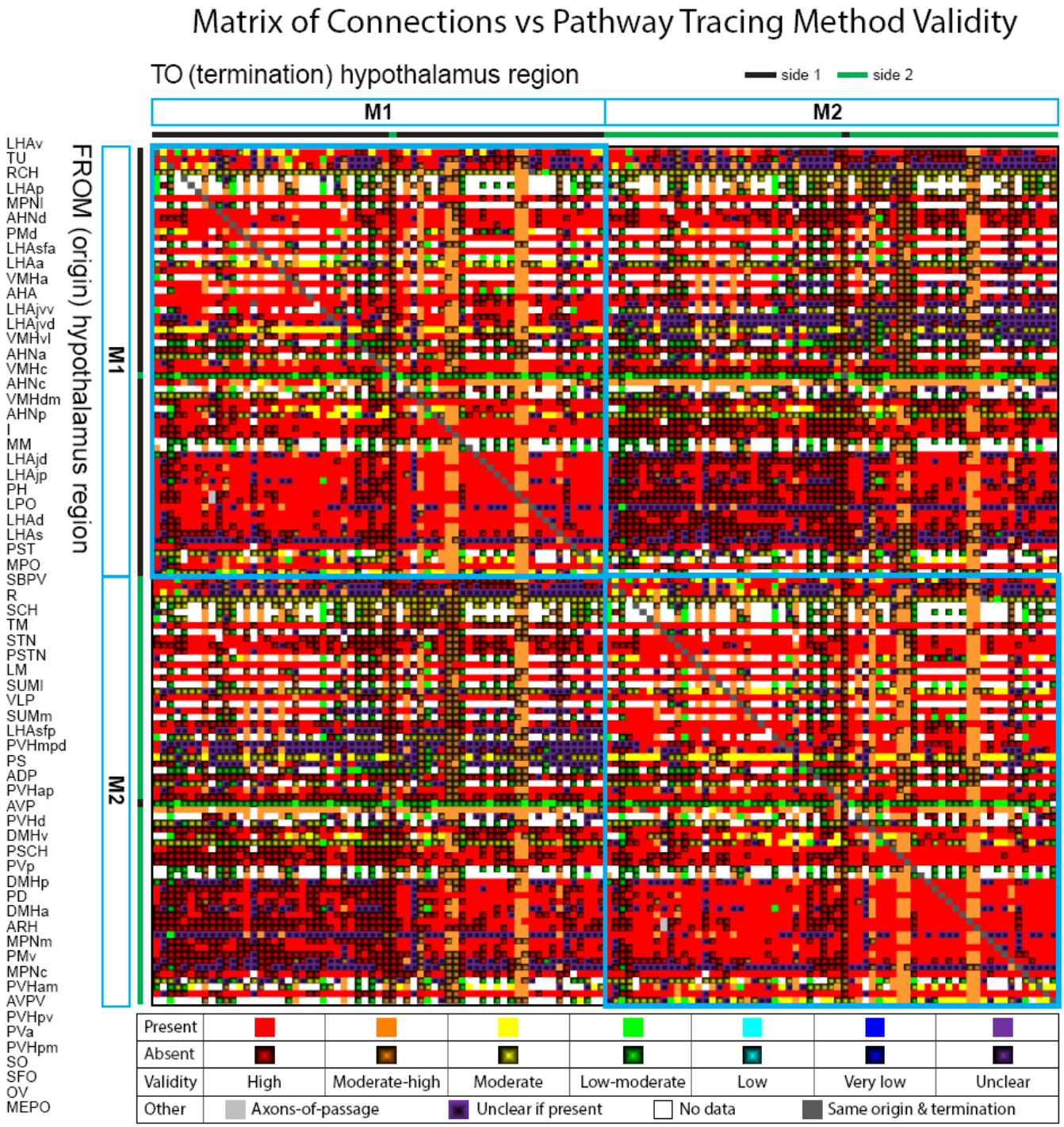

Fig. S1. Comparative matrix of connections and validity of pathway tracing methods. The matrix combines a weighted connection matrix for the bilateral intrahypothalamic subconnectome with a measure of the validity of the experimental pathway tracing methods for present and absent connections, based on a seven-point scale. Note that for connections reported as absent, a lower pathway tracing method validity does not necessarily reduce the validity of the data (see methodological discussion in ref. 1). Region arrangement is determined by the results of multiresolution consensus clustering analysis (Fig. 2) (2). Region abbreviations are defined in Dataset S2.

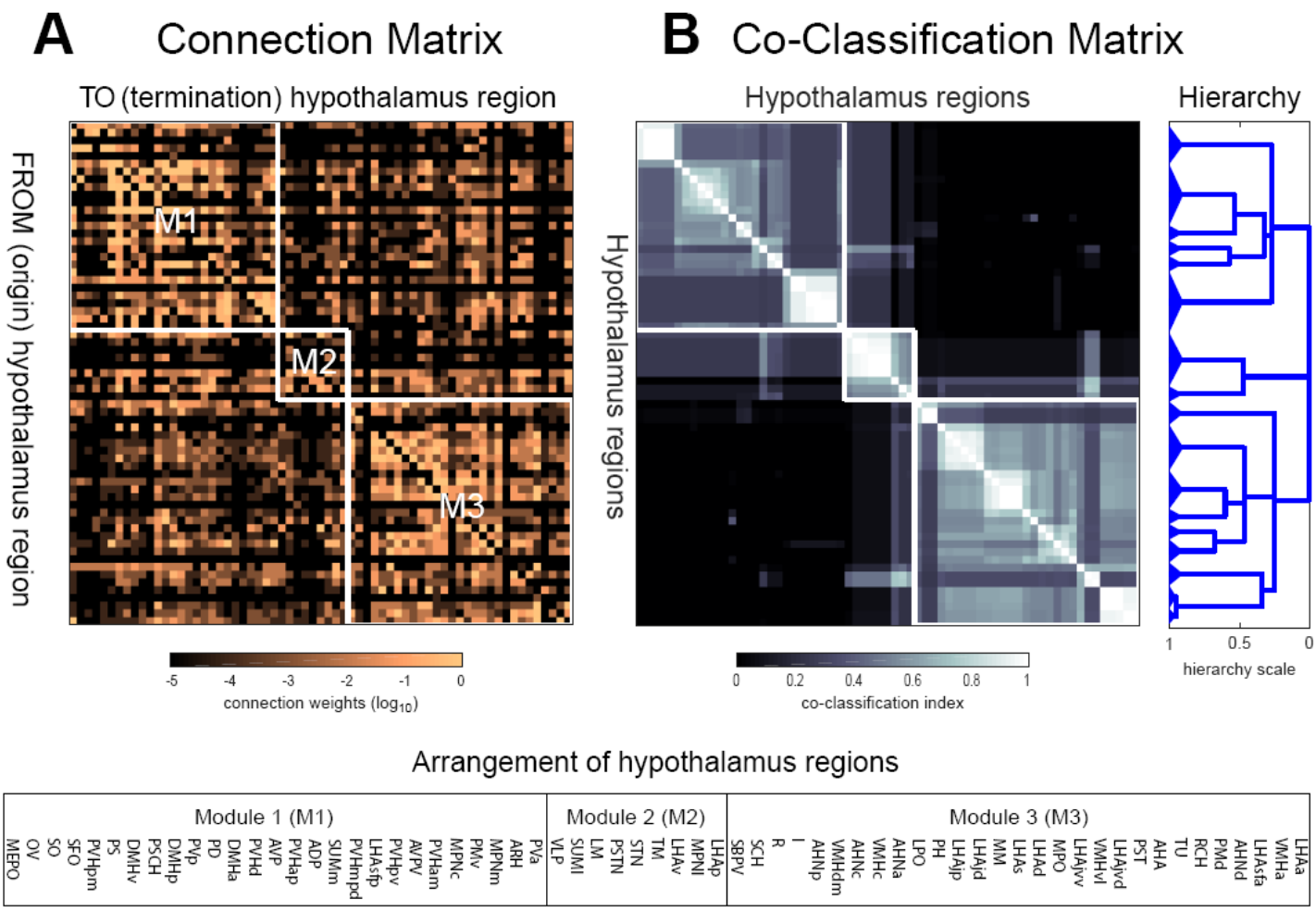

Fig. S2. Connection and co-classification network matrices for the unilateral intrahypothalamic (HY1) subconnectome. (*A*) Directed and weighted monosynaptic macroconnection matrix for the rat hypothalamus on one side (unilateral, HY1) with gray matter region sequence in a subsystem arrangement derived from a multiresolution consensus clustering (MRCC) analysis strategy (shown in *B*) (2). Connection weights are represented on a $\log_{10}$ scale. Three top-level subsystems (modules M1-3) are outlined in white. (*B*) Complete co-classification matrix obtained from MRCC (as in *A*) for the 65 regions of the hypothalamus on one side. A linearly scaled co-classification index (below) gives a range between 0 (no co-classification at any resolution) and 1 (perfect co-classification across all resolutions). Ordering and hierarchical arrangement are determined after building a hierarchy of nested solutions (100,000 event samples) that recursively partition each cluster/subsystem (as in Fig. 2), starting with the three top-level clusters/subsystems (i.e. M1-3). All solutions plotted in the tree survive the statistical significance level of $\alpha = 0.05$. Region abbreviations are defined in Dataset S2.

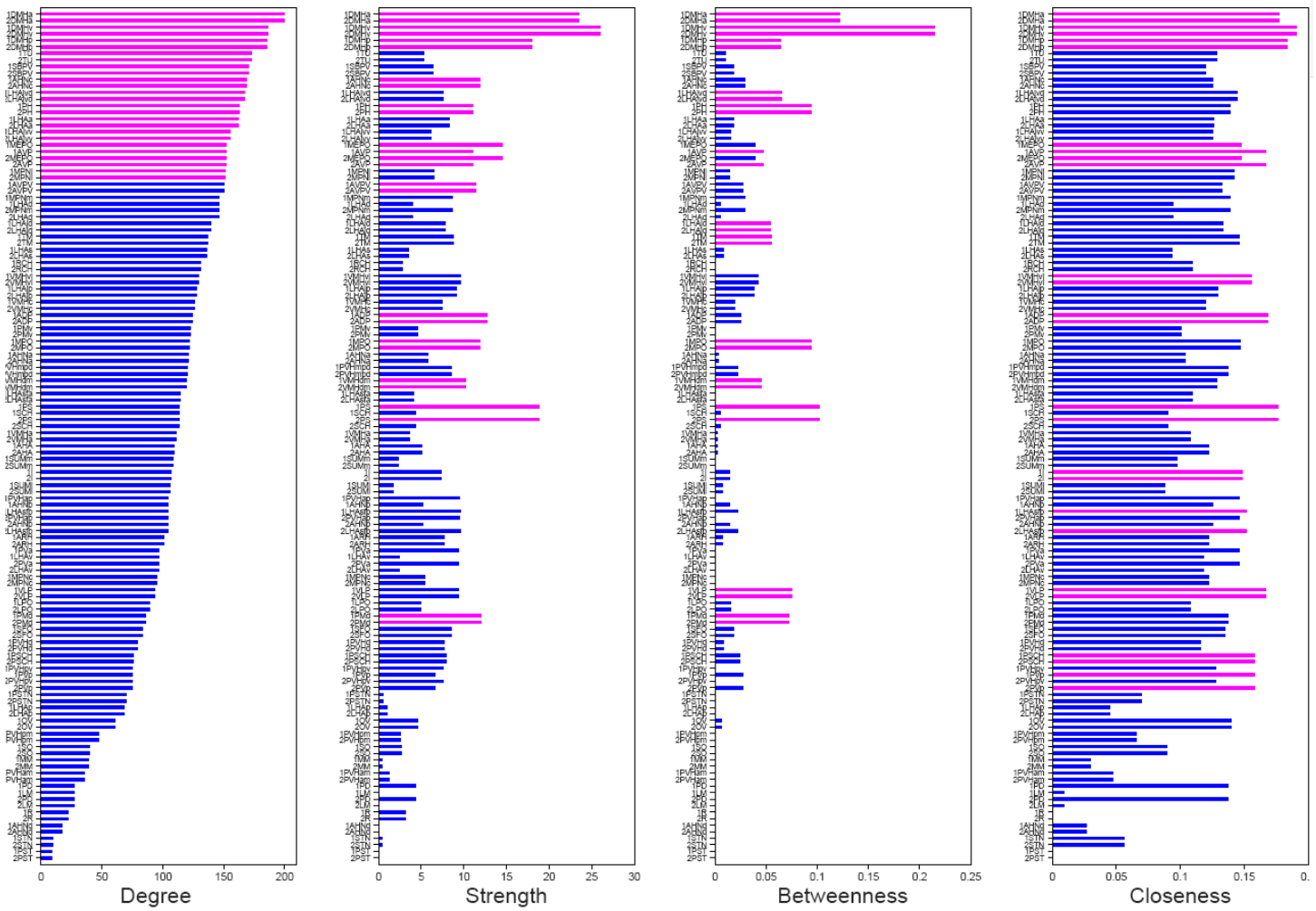

Fig. S3. Centrality metrics for all regions of the bilateral intrahypothalamic subconnectome. Rankings of 65 hypothalamic regions (applied to each side) according to four centrality measures: Degree, Strength, Betweenness, and Closeness. Regions are ranked by degree across all four plots, with regions in the top 20th percentile (including tied values) for each measure indicated by pink (magenta) bars.

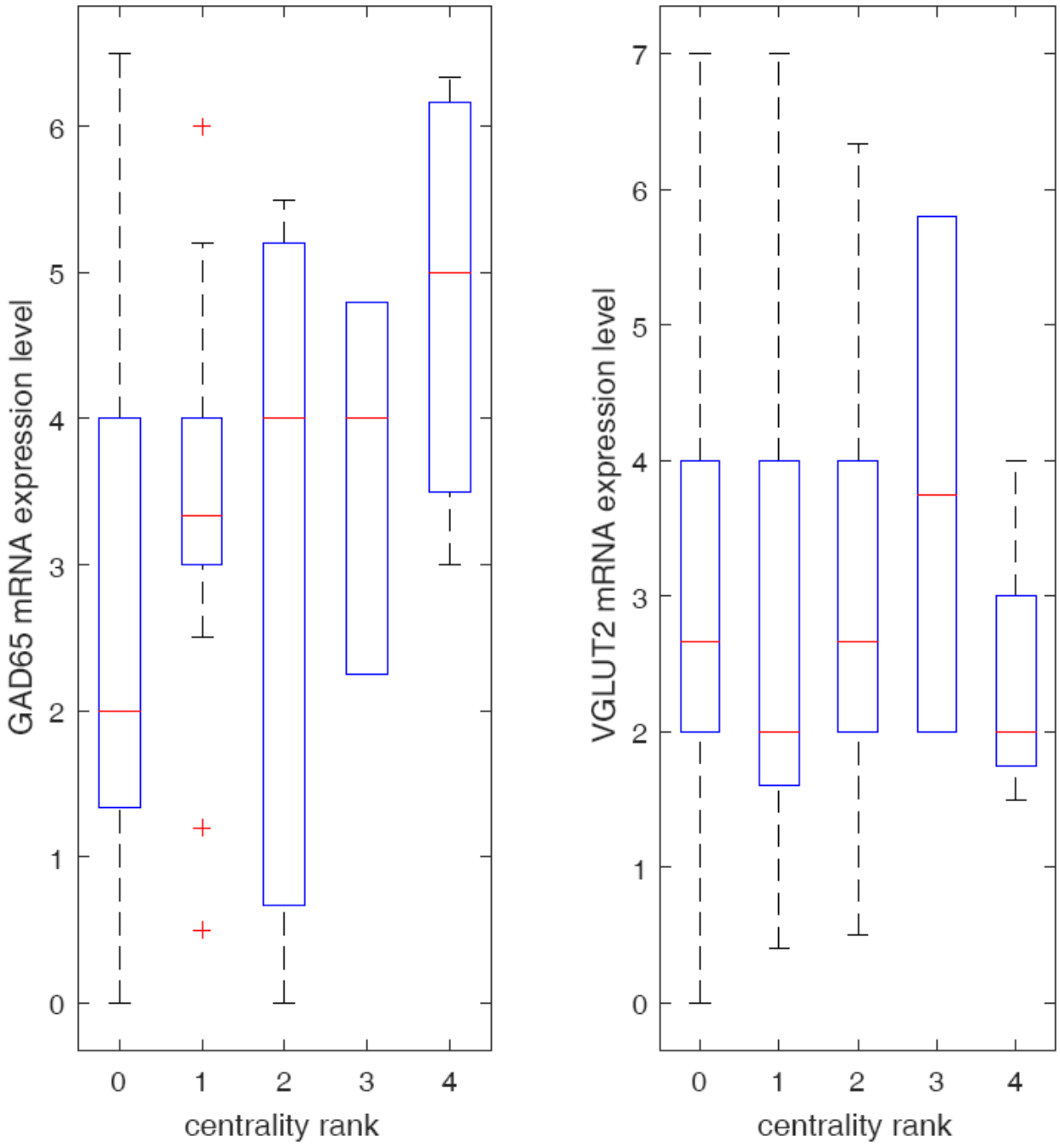

Fig. S4. Comparison of centrality for the intrahypothalamic network, with GAD65 and VGLUT2 mRNA expression. Hypothalamus regions are arranged into five groups, according to their aggregated centrality score (0, 1, 2, 3, 4) in the intrahypothalamic network across four different measures of node centrality (degree, strength, betweenness, closeness; see Fig. 4 and S3). Regions with a score of 4 are most central, while regions with a score of 0 are least central in the network. The box plot summarizes the group-wise distributions of gene expression levels for GAD65 (left panel) and VGLUT2 (right panel). Red line indicates median, box indicates 25th (lower margin) and 75th (upper margin) percentile, whiskers indicate upper and lower range, red crosses indicate values considered outliers. Note the progressive increase in median GAD65 expression with centrality rank and the lack of such increase with VGLUT2 expression (for region-wise Spearman correlations see main text).

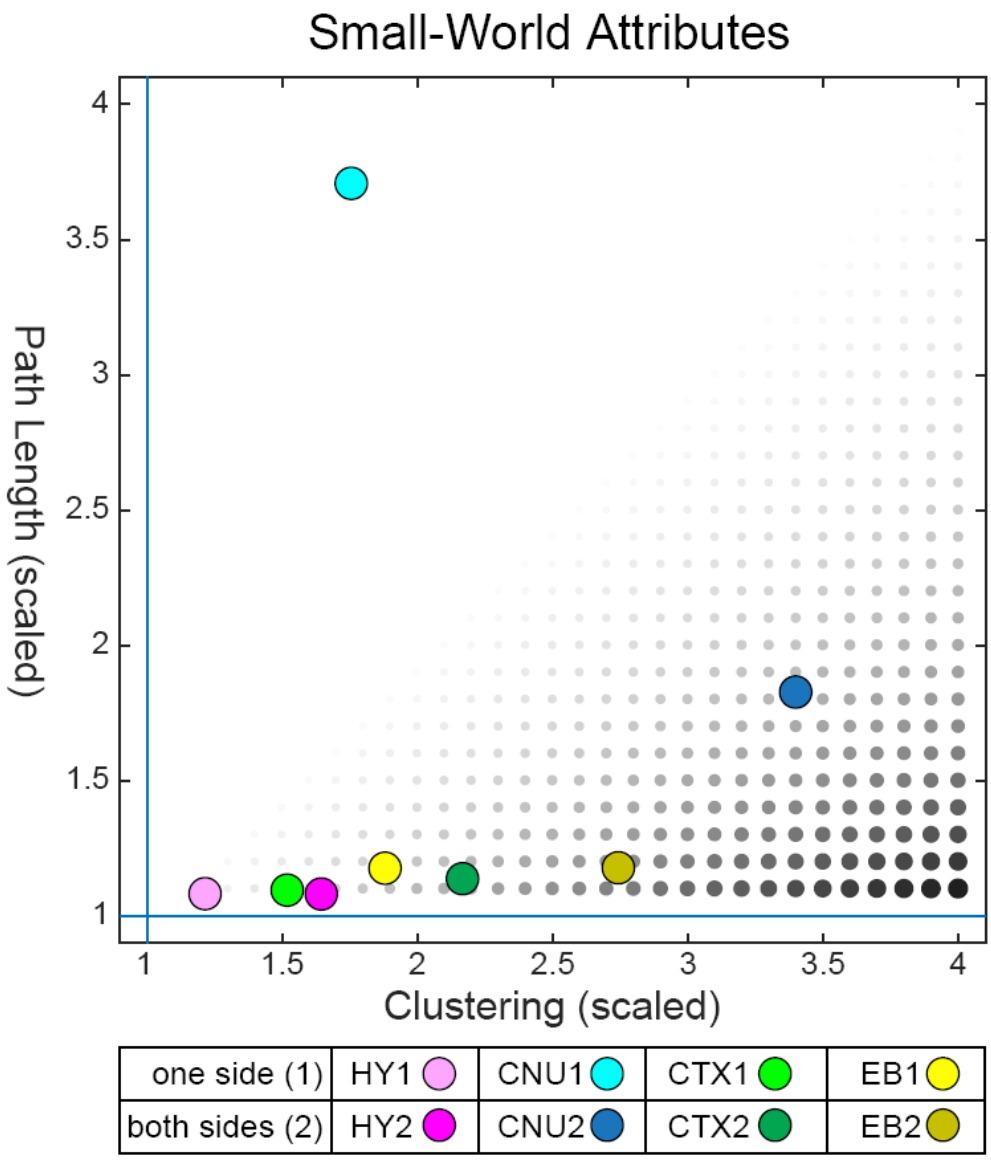

Fig. S5. Weak small-world attributes for the intrahypothalamic network. *Small-world* networks possess the dual properties of having nodes that are highly clustered (densely interconnected) and connected by short paths. Clustering is computed as the nodal mean of the weighted and directed clustering coefficients, and path length is computed as the global mean of the weighted path lengths between all node pairs. Both metrics are scaled by the median of the corresponding measures obtained from 1,000 degree-preserving randomized networks. The size and gray level of black symbols correspond to the ratio between scaled clustering and scaled path length, the small-world index (3). For a network to possess *small-world* attributes, this index should be >1, with a high (scaling >> 1) clustering index and a short (scaling near 1) path length. The overall path length for the bilateral (HY2) and unilateral (HY1) hypothalamic macroscale subconnectomes was close to 1, and the clustering values were ~1.2 for HY1 and ~1.7 for HY2. HY1 meets only 1 of the 2 criteria required for the *small-world* attribute; whereas HY2 (with the addition of contralateral connections) is slightly more clustered, conferring a marginal *small-world* attribute. For comparison, values are also plotted for previously reported subconnectomes for the endbrain (EB1 & 2) (1), and its component parts the cerebral cortex (CTX1 & 2) (4), and cerebral nuclei (CNU1 & 2) (5). It is noteworthy that the subconnectomes CNU2, CTX2, and EB2 all show more robust *small-world* attributes than HY2.

Additional Dataset S1 (separate file). The complete list of collated macroconnection reports for the rat hypothalamus that was used to compile a dataset for network analysis of the intrahypothalamic macroscale subconnectome (Microsoft Excel Worksheet file). The sequence of tabulated macroconnection reports follows the topographic arrangement of regions in a canonical rat brain reference atlas (6). When multiple connection reports for a macroconnection of interest were found, the one considered to be most valid was selected for network analysis. Abbreviations for pathway tracers: ARGM, autoradiographic method; BDA, biotinylated dextran amine (MW. 3,000 or 10,000); CTB, cholera toxin B subunit; CTB-gold, CTB conjugated to colloidal gold; CTB-HRP, CTB conjugated to horseradish peroxidase; HRP, horseradish peroxidase; PHAL, *Phaseolus vulgaris*-leucoagglutinin; rAAVirus-GFP, recombinant adeno-associated viral vector (rAAV) expressing green fluorescent protein (GFP); WGA-apoHRP-Gold, wheat germ agglutinin apoHRP gold.

Additional Dataset S2 (separate file). Data matrices for the intrinsic macroconnections of the rat hypothalamus (Microsoft Excel Worksheet file). Data were extracted from macroconnection reports in the primary literature (see Dataset S1). The Excel file has 5 worksheets. The first worksheet provides an annotated list of connection report weight categories, their abbreviations, and correspondence between these terms and their assigned numerical value for collated (raw) and binned data (see Analysis Framework section of the Results for details). Worksheets 2-5 provide rat hypothalamus macroconnection data (separate sheets for binned and raw data) in two arrangements: 1) in a subsystem arrangement determined by a multiresolution consensus clustering method (2) applied to the bilateral hypothalamic subconnectome (worksheets 2 and 3), with top level subsystems or modules highlighted (see also Fig. 2*A*, 3), and 2) in a topographic arrangement (worksheets 4 and 5), according to a rat brain reference atlas (6). Matrix directionality for the data worksheets (2-5) is from y-axis to x-axis.

Additional Dataset S3 (separate file). Raw data from analysis of GAD65 and VGLUT2 mRNA expression in the rat hypothalamus (Microsoft Excel Worksheet file). Analysis of GAD65 and VGLUT2 mRNA expression in the rat hypothalamus was performed on separate series of rat brain sections for each gene marker, labeled by isotopic *in situ* hybridization (see Methods for further information). An ordinal value ranging from 1 (*very weak*) to 7 (*very strong*) was assigned to each region on one side of the brain for each available level of its representation in a rat brain reference atlas (6), to give an average value for each region.

References for Supporting Information.

1. Swanson LW, Hahn JD, Jeub LGS, Fortunato S, & Sporns O (2018) Subsystem organization of axonal connections within and between the right and left cerebral cortex and cerebral nuclei (endbrain). *Proc Natl Acad Sci U S A.* 115(29):E6910-E6919.
2. Jeub LGS, Sporns O, & Fortunato S (2018) Multiresolution Consensus Clustering in Networks. *Sci Rep* 8(1):3259.
3. Humphries MD & Gurney K (2008) Network 'small-world-ness': a quantitative method for determining canonical network equivalence. *PloS one* 3(4):e0002051.
4. Swanson LW, Hahn JD, & Sporns O (2017) Organizing principles for the cerebral cortex network of commissural and association connections. *Proceedings of the National Academy of Sciences of the United States of America* 114(45):E9692-E9701.
5. Swanson LW, Sporns O, & Hahn JD (2016) Network architecture of the cerebral nuclei (basal ganglia) association and commissural connectome. *Proceedings of the National Academy of Sciences of the United States of America* 113(40):E5972-E5981.
6. Swanson LW (2018) Brain maps 4.0-Structure of the rat brain: An open access atlas with global nervous system nomenclature ontology and flatmaps. *The Journal of comparative neurology* 526(6):935-943.